You are as fast as your motor neurons: Speed of recruitment and maximal discharge of motor neurons determine the maximal rate of force development in humans

A. Del Vecchio[1,4], F. Negro[2], A. Holobar[3], A. Casolo[1, 4], J.P. Folland[5], F. Felici[4], D. Farina[1]

Affiliations

[1]Department of Bioengineering, Imperial College London, SW7 2AZ, London, UK.

[2]Department of Clinical and Experimental Sciences, University of Brescia, Brescia, Italy.

[3]Faculty of Electrical Engineering and Computer Science, University of Maribor, Slovenia.

[4]Department of Movement, Human and Health Sciences, University of Rome "Foro Italico", Rome, Italy.

[5]School of Sport, Exercise & Health Sciences, Loughborough University, Loughborough, UK.

Corresponding author:

Dario Farina. Department of Bioengineering, Imperial College London, SW7 2AZ, London, UK. Tel: Tel: +44 (0)20 759 41387, Email: d.farina@imperial.ac.uk

Abbreviated title: You are as fast as your motor neurons

Keywords: Motor unit; Neural Drive; Spike frequency adaptation; Ballistic contractions; EMG Decomposition

Key points:

- We propose and validate a method to accurately identify the activity of populations of motor neurons during contractions at maximal rate of force development in humans.
- The behaviour of the motor neuron pool during rapid voluntary contractions in humans is presented.
- We show with this approach that the motor neuron recruitment speed and maximal motor unit discharge rate largely explains the individual ability in generating rapid force contractions.
- The results also indicate that the synaptic inputs received by the motor neurons before force is generated dictate human potential to generate force rapidly.
- This is the first characterization of the discharge behaviour of a representative sample of human motor neurons during rapid contractions.

Abstract

During rapid contractions motor neurons are recruited in a short burst and begin to discharge at high frequencies (up to >200 Hz). Here we studied the behaviour of relatively large populations of motor neurons during rapid (explosive) contractions in humans applying a new approach to accurately identify motor neuron activity simultaneous to measuring rate of force development. The activity of spinal motor neurons was assessed by high-density EMG decomposition from the tibialis anterior muscle of 20 men during isometric explosive contractions. The speed of motor neuron recruitment and the instantaneous motor unit discharge rate were analysed as a function of the impulse (the time-force integral) and the maximal rate of force development. The peak of motor unit discharge rate occurred before force generation and discharge rates decreased thereafter. The maximal motor unit discharge rate was associated to the explosive force variables, at the whole population level (R^2 = 0.71 (0.12), P<0.001). Moreover, the peak motor unit discharge and maximal rate of force variables were correlated with an estimate of the supraspinal drive, that was measured as the speed of motor unit recruitment before the generation of afferent feedback (P<0.05). We showed for the first time the full association between the effective neural drive to the muscle and human maximal rate of force development. The results obtained in this study indicate that the variability in the maximal contractile explosive force of the human tibialis anterior muscle is determined by the neural activation preceding force generation.

Introduction

When the central nervous system requires maximal speed and force, motor neurons discharge at frequencies that are significantly greater compared to sustained contractions (up to 200 Hz vs.10-40 Hz) (Desmedt & Godaux, 1977*a*; Freund, 1983). Voluntary force contractions at maximal rate of force development indeed provide access to the maximal in-vivo motor neuron discharge rate in humans (Desmedt & Godaux, 1978; Duchateau & Baudry, 2014). In these contractions, the neural drive to the muscle during the initial phase of the motor task, i.e. during the neuromechanical delay, represents the effect of cortical input to motor neurons without the afferent feedback generated by the contracting muscle. During these rapid (explosive) contractions, the ordered recruitment is maintained but most motor units are recruited before the rise in force (Tanji & Kato, 1973; Büdingen & Freund, 1976; Desmedt & Godaux, 1977*b*; Van Cutsem *et al.*, 1998). It is known that recruitment and increase in discharge rate determines the rate of change in force (Desmedt & Godaux, 1977*b*; Freund, 1983; Enoka & Duchateau, 2017). However, it is not known whether the extensive variability among individuals (Folland *et al.*, 2014) in maximal rate of force development is determined by motor unit properties. This raises the question: are human movements as fast as the driving motor neurons?

It has been recently speculated that the maximal motor neuron discharge rate may determine the rate of force development (Duchateau & Baudry, 2014). When electrically stimulating muscles, the contractile rate of force development of a muscle indeed depends on the stimulation frequency in the rat (de Haan, 1998) and human muscle (Deutekom *et al.*, 2000). Moreover, following three months of fast ballistic training, the increase in rate of force development is paralleled by an increase in motor unit discharge rate in humans (Van Cutsem *et al.*, 1998). Further, ageing decreases the discharge rate of motor neurons and concurrently the rate of force development (Klass *et al.*, 2008). Simulation studies seem to support an association between motor neuron discharge rates and rapid force production but there are no direct experimental observations for this association (Fuglevand *et al.*, 1993; Harwood & Rice, 2012). Moreover, the variability of motor neuron behaviour across individuals during maximal rate of force development is unknown.

Because of technical challenges in tracking motor unit action potentials during the maximally rising phase of contraction, the neural drive to the muscle during contractions at maximal rate of force development has been characterized only for the initial phase of the contractions (first four motor unit action potentials, ~40-60 ms) (Desmedt & Godaux, 1977*b*; Van Cutsem *et al.*, 1998; Van Cutsem & Duchateau, 2005) or in in-vitro

studies when injecting current in the motor neurons (Granit *et al.*, 1963; Sawczuk *et al.*, 1995; Miles *et al.*, 2005). The time-course of the discharge rate of motor neurons during explosive contractions is unknown. Moreover, the number of motor units identified per subject in previous studies was very small (1-2) and not representative of the effective neural drive to the muscle. In this study, we estimated the neural drive to the muscle during explosive contractions by identifying the concurrent activity of a relatively large number of motor neurons (>10 per subject). The aim was to assess the association between the behaviour of motor neurons and the capacity for rapid force production. We hypothesized that the speed of recruitment and the maximal generated discharge activity of the motor neuron pool would determine the human maximal rate of force development.

Materials and methods

Participants and recruitment

Twenty healthy, recreationally active men (24.9 (3) yr, 75.4 (8.6) kg, 180 (10) cm, 2636 (1298) metabolic equivalent min/wk (IPAQ) volunteered to participate in the experiment, which was approved by the Ethical Committee of the University of Rome “Foro Italico” (approval n. 44680) and conformed to the standards set by the Declaration of Helsinki. The volunteers were free from any neuromuscular disorder, lower limb pathology or surgery and not involved in any form of regular physical training. A written informed consent was signed by the volunteers.

Overview of the study

The volunteers visited the laboratory on two occasions seven days apart. Before the first visit, the recreational physical activity habits of the participants were assessed using the International Physical Activity Questionnaire (IPAQ, short format). The first visit consisted of a familiarization session including both maximal and explosive voluntary contractions of the dominant leg (self-reported). The contractions consisted of isometric ankle dorsi-flexion maximal voluntary contractions (MVC), isometric short pulsatile contractions, and isometric explosive force contractions. In the second visit, the participants repeated the familiarization session but with recording of EMG activity with high-density surface electromyography (HDsEMG) of the tibialis anterior muscle. Participants were asked to avoid any strenuous exercise (48 hours) and caffeine consumption (24 hours) before the testing sessions.

Experimental procedure

The warm-up consisted of 8 isometric submaximal dorsi-flexions (4 x 50%, 3 x 70%, 1 x 90% of perceived maximal voluntary force), each separated by 15 s, and a series of short pulsatile contractions. During the short pulsatile contractions the volunteers were instructed to contract as fast as possible up to a target force of 75% of the maximal voluntary force (MVF) (defined below) displayed on the screen, and relax immediately after the peak force was reached (Van Cutsem *et al.*, 1998). The short pulsatile contractions were used to familiarise the participants with developing force as quickly as possible, and to confirm that the RFD measured during the explosive contractions used for decomposition analysis was indeed maximal. After the warm-up, the subjects performed isometric MVCs and isometric maximal explosive contractions. During the MVCs the participants received strong verbal encouragement and were instructed to "push as hard as possible" for 3-5 s, with ≥30 s rest in between, for a total of three repetitions. Visual feedback of the exerted force in each contraction and that of the maximal previous contractions was provided. The greatest dorsi-flexors MVF corresponding to the highest instantaneous force during the MVCs was digitally recorded. After 4 min from the completion of the MVCs the volunteers performed 12 isometric explosive dorsi-flexions that were divided into two blocks of six repetitions each. Each contraction was separated by a resting period of 20 s and a 2-min rest was provided after each block. The volunteers were instructed to dorsi-flex their ankle "as fast and as hard as possible" and to exceed a visual target cursor on the monitor, fixed at a threshold of 75% of their MVF, and then hold the force for 3 s at the same level reached during the explosive contraction. Explosive contractions were performed as a maximum explosive force production followed by an hold phase in order to increase the contraction duration, as needed by the decomposition algorithm for identifying a sufficient number of independent sources (motor unit action potentials) from the electromyogram (Holobar *et al.*, 2014; Negro *et al.*, 2016). Moreover, the inclusion of a hold phase following the explosive effort allowed validation of the decomposition approach during the rapid part of the contraction (see "High-density EMG analysis"). The beginning of each explosive contraction was indicated with an auditory cue. The participants were instructed to avoid any counter movement or pre-tension, and a feedback was given when an error was detected. Offline analysis confirmed large agreement in the maximal rate of force development obtained during the short pulsatile contractions and the explosive contractions.

Force signal recording

A stiff custom-built ankle ergometer was used both in the familiarization and in the main experiment (OT Bioelettronica, Turin, Italy) and guaranteed a high stiffness during the explosive contractions. Participants were comfortably seated with the hip flexed at ~120° (180° = anatomical position) on a massage table with

the dominant knee extended at ~180° (180° = anatomical position) and the ankle at ~100° (90° = anatomical position) of plantar flexion. The foot rested on an adjustable footplate and along with the ankle was tightly harnessed by Velcro straps. The foot strap (~3 cm wide) was positioned over the distal portion of metatarsals, while the ankle strap (~3 cm wide) was fastened on the foot dorsum, perpendicular to the tibia. The foot strap was arranged in series with a calibrated load cell (CCT Transducer s.a.s, Italy), which was positioned perpendicular to the plantar surface of the foot. The analogue force signal from the load cell was amplified (x200) and sampled at 2048 Hz through an external analog-to-digital (A/D) converter (EMG-Quattrocento, OT Bioelettronica, Turin, Italy). The force signal was recorded with the software OTbiolab (OT Bioelettronica, Turin, Italy) and the visual feedback was provided with Labview 8.0 (National Instruments, Austin, USA).

High-density surface electromyography recordings (HDsEMG)

HDsEMG signals were recorded from the tibialis anterior muscle with one semi-disposal adhesive grid of 64 equally spaced electrodes (13 rows x 5 columns; gold-coated; diameter: 1-mm; inter electrode distance (IED): 8-mm; OT Bioelettronica, Turin, Italy). Following skin preparation (shaving, gentle skin abrasion and cleansing with 70% ethyl alcohol), the optimal position and orientation of the matrix were determined. For this purpose, an experienced operator identified the tibialis muscle belly through palpation and marked the perimeter of the muscle with a surgical pen. Then, the adhesive grid was placed over the muscle using bi-adhesive perforated foam layers (SpesMedica, Battipaglia, Italy). A conductive paste was inserted in the bi-adhesive layer in order to guarantee good skin-electrode contact (SpesMedica, Battipaglia, Italy). The grid covered most of the tibialis anterior proximal area. The ground electrode was placed on the styloid process of the ulna of the arm, and two reference electrodes were positioned on the tuberositas tibialis and on the medial malleolus of the dominant leg. The HDsEMG signals were detected in monopolar mode with a sampling frequency of 2048 Hz, amplified *(x* 150*)* and band-pass filtered (10-500 Hz). The analog signals were converted to digital data by a multichannel amplifier with a 16-bit resolution (3-dB bandwidth, 10-500 Hz; EMG-Quattrocento, OT Bioelettronica, Turin, Italy). The electromyogram and force signal were synchronized by the same acquisition system.

High density EMG analysis

During offline analysis, the monopolar HDsEMG signals were band pass filtered at 20-500 Hz (Butterworth). The EMG signals were decomposed in individual motor unit action potentials (MUAPs) by convolutive blind source separation (Holobar & Zazula, 2007). This method and similar approaches have been previously validated for a broad range of forces of the tibialis anterior muscle and guarantees high accuracy in the identification of motor unit spike trains (Holobar *et al.*, 2014; Negro *et al.*, 2016; Del Vecchio *et al.*, 2017). The decomposition accuracy was assessed using the pulse to noise ratio (Holobar *et al.*, 2014). All motor units were manually analysed by an experienced investigator and only MUAPs with a reliable discharge pattern were considered for the analysis. Motor units showing pulse to noise ratios <30 dB were discarded from the analysis (Holobar *et al.*, 2014).

The decomposition accuracy during the explosive contractions was further assessed with additional analyses, needed to prove the accuracy during these explosive contractions. In one single decomposition, we first decomposed the three explosive contractions with the highest force reached at 150 ms from contraction onset out of the 12 contractions performed by each subject. This criterion facilitated systematic selection of contractions with both high rate of force development and large time-force integral, since the plateau of the force time-curve occurs before 200 ms from force onset and thus well approximates the peak of the derivative and the time-force area. Successively, we identified motor units active across these three explosive contractions. In a separate decomposition, we processed one of the same three contractions, randomly chosen. From this decomposition, the MUAP waveforms identified by blind source separation were used as spatial filters to identify the discharge patterns of the same waveforms in the other two contractions, which were not decomposed. By comparing the extracted motor units when decomposing the three contractions together and separately, we tested the reliability of the decomposition algorithm to identify the same motor units across the three contractions. All motor units with a 95% match of the series of discharge timings were considered reliably identified. Further, because during the explosive contractions the initial discharge rates of the motor units are very high (up to 200 Hz, e.g., Fig. 1C, Desmedt and Godaux, 1977b; Van Cutsem et al., 1998), we assessed the similarity (by cross-correlation analysis) of the action potential waveform shapes during the initial phase of the contraction (the first 20 motor unit discharges) compared to those extracted during the steady state (using the last 50 motor unit discharges of the contraction). Since the decomposition accuracy during static contractions has been previously proven (Holobar *et al.*, 2014), the comparison with the transient rapid force rise provided another indirect validation of the technique during explosive contractions. For this purpose, we computed the two dimensional cross-correlation between the

decomposed MUAPs in the two phases of the contractions (Farina *et al.*, 2002; Del Vecchio *et al.*, 2017; Martinez-Valdes *et al.*, 2018).

From all the identified motor units, the maximal instantaneous discharge rate (DR_{MAX}, pulses per second, pps), recruitment threshold in %MVF, and the cumulative spike trains (Del Vecchio *et al.*, 2018*d*) were calculated. The time span of recruitment was defined as the time interval containing the first discharges of all identified motor units. Finally, the speed of recruitment was defined as the inverse of the time span of recruitment, which corresponded to the average number of identified units that were recruited per second. It is important to note that the above definitions for characterizing recruitment are related to the sample of identified motor units and not to all recruited units.

The cumulative spike train was obtained by summing the discharge timings of the identified motor units. The cumulative spike train was analysed in time intervals of 35-ms duration. This interval duration was chosen because it approximately corresponded to the neuromechanical delay (see Results) and thus it allowed the analysis of the neural drive before force generation. The 35-ms analysis window was shifted over time with increments of 1 ms in a total range of 250 ms from the onset of motor unit activity. The analysis was limited to 250 ms because most of the changes in rate of force development during isometric explosive contractions occur before ~150 ms following force onset (Del Vecchio *et al.*, 2018*b*). In each 35-ms interval, the total number of discharges in the cumulative spike train was divided by the number of active motor units and by the window duration (35 ms), providing the average number of discharges per motor unit per second (DR_{MEAN}). This measure is an estimate of the strength of the neural drive to the muscle (Del Vecchio *et al.*, 2018*d*). Figure 1 shows an example of this analysis that extracted the instantaneous and average number of discharges per motor unit per second (as explained above) obtained during an explosive contraction.

To globally characterise the EMG signal amplitude, the root mean square value was computed from one bipolar recording derived from the HDsEMG signals. Specifically, two sets of five neighbouring monopolar signals within the central portion of the HDsEMG (columns 2-4 and rows 4-7 of the bidimensional array) were averaged and differentiated in order to obtain a bipolar EMG derivation with an equivalent interelectrode distance of 1.6 cm (Del Vecchio *et al.*, 2017, 2018*a*). From this signal, the root mean square value was estimated in the same time intervals used for assessing the motor unit properties. Finally, the root mean square value was also normalized to the maximal value obtained at maximal voluntary force (i.e. a 100-ms time period centred at MVF during MVC).

Force signal analysis

During offline analysis, the force signal was converted to Newton (N) and the offset of force was gravity corrected. The contractions that showed pre-tension or countermovement (baseline force ≥ 0.5 N in 150 ms prior to force onset) were excluded. The force signal was filtered with a zero-lag low-pass filter with cut-off frequency 400 Hz. This large bandwidth guarantees high accuracy when visually determining the onset of force (Tillin *et al.*, 2013). The onset of force was visually identified by an experienced investigator with a validated methodology, previously described (Tillin *et al.*, 2010). After identifying the force onset, the signal was low-pass filtered at 20 Hz with a zero-lag 3rd order Butterworth filter. This type of filter eliminates the high-frequency noise and guarantees an undistorted force output in comparison to the original signal (Del Vecchio *et al.*, 2018*b*). Out of the explosive contractions performed by each subject and without initial tension, only the three contractions with the highest force at 150 ms from force onset were selected for the full analysis, as described previously. For these three contractions, the force signal was analysed in the 250-ms interval following force onset. For each overlapping time interval from force onset, the first derivative of force was then calculated (i.e. RFD 0(onset) to X ms, where X varied in the range 1-250 ms) in order to identify the maximal rate of force development (RFD0-$X_{MAX,}$ N/s). The RFD was also computed for specific time periods from force onset to 60 (RFD0-60) and to 100 (RFD0-100) ms because previous studies suggested a stronger neural contribution during this phase of contraction (~0-100 ms) (de Ruiter *et al.*, 2007; Folland *et al.*, 2014) and also to investigate fixed/consistent time periods for all participants. Moreover, the integral of the force-time curve, i.e. the impulse (N*s), was calculated in the interval from force onset to 250 ms and thus reflected the entire time history of the contraction. Because the impulse is proportional to the change in momentum (mass * change in velocity), it is directly associated to the change in velocity and thus to the ankle dorsiflexion speed if the foot was not restrained by the dynamometer (Aagaard *et al.*, 2002). Beside absolute explosive force variables (RFD, impulse), relative measures reflect the ability of participants to explosively express their available force capacity (MVF) quickly during the rising phase of contraction (i.e., RFD/impulse normalised to MVF) (Folland *et al.*, 2014; Del Vecchio *et al.*, 2018*b*).

Statistics

The Shapiro-Wilk test showed a normal distribution of all extracted variables. The Bonferroni correction was used when testing multiple correlations. DR_{MAX} and DR_{MEAN} (hereafter referred to as neural variables) were analysed in relation to the absolute and normalized force values (RFD0-X_{MAX}, RFD0-60, RFD0-100, and Impulse). The motor unit recruitment speed was studied as a function of the neural drive estimates and

277 explosive force. The initial values and consecutive values of the neural estimates were assessed as a
278 function of the force values with multiple correlations. The motor unit recruitment thresholds were analysed
279 as a function of the average motor unit discharge rate and rate of force development. The rate of force
280 development during the first 60 and 100 ms was then studied as a function of the impulse. The strength of
281 the neural drive to muscle, estimated as the average number of discharges per unit per second, was
282 compared between the first 60 ms of contraction and the steady force part of the contraction with a paired t-
283 test. The waveforms of the motor unit action potentials between and within contractions were assessed by a
284 two-dimensional cross-correlation function (xcorr2, MATLAB 2017, MathWorks Inc.). The coefficient of
285 variation (standard deviation of the population (SD) divided by the mean) was assessed for the force and the
286 motor unit discharge interpulse interval. A Pearson product-moment correlation was used to assess the
287 strength of bivariate correlations. Significance was accepted for P values smaller than 0.05. Data are
288 reported as mean (SD).

289 **Results**

290 *Force*

291 Figure 1 shows the time-force curve for a representative subject and Figure 2 the explosive force variables
292 for each subject. Each colour in Figure 2 represents an individual subject. The maximal rate of force
293 development had inter-subject coefficient of variation of 30.0% and 19.2% for the absolute and normalized
294 RFD0-XMAX, respectively. The impulse (0-250 ms) had a coefficient of variation of 24.4 and 12.4% across
295 subjects, for the absolute and normalized values respectively. The maximal isometric voluntary force ranged
296 from 166.72 to 364.88 N across subjects, with an average of 278.10 (58.34) N and a coefficient of variation
297 of 20.0%. The maximal voluntary force was highly correlated with the RFD_{MAX} and Impulse (R^2 =0.62 (0.12),
298 Pearson-P <0.001).

299 The delay between the first detected motor unit action potential and the onset of voluntary force, i.e. the
300 neuromechanical delay, was on average 42.4 (17) ms.

301 *Motor unit analysis validation*

302 Only motor units showing reliable discharge patterns with a pulse-to-noise ratio greater than 30 dB (Holobar
303 *et al.*, 2014) were selected for the analysis. The total number of decomposed motor units was 242, with an

304 average of 12.1 (5.7) per subject. Figure 1 shows the identified motor unit discharge timings during a
305 representative explosive force contraction. The MUAP waveforms were cross-correlated between and within
306 contractions. The within-contraction correlation represents the degree of similarity of MUAPs of the first 20
307 discharges when compared to the first 50 discharges during the steady force phase (Fig. 3C). The average
308 two-dimensional coefficient of correlation across subjects in this comparison was R = 84.3 ± 8.0 (%). The
309 discharge timings of a representative motor unit and the respective MUAP waveforms are shown in Fig. 3A-
310 C. When the pool of identified motor units was cross-correlated across the three explosive contractions (Fig.
311 3B-D), the average coefficient of correlation (average over all subjects) was 88.4 ± 3.0 (%). The discharge
312 pattern and estimated action potential waveforms were highly similar when compared across the three
313 maximal explosive contractions (an example is shown in Fig. 3D). The two-dimensional correlation was also
314 evaluated for randomly selected motor units between each contraction and the estimated value was very low
315 (30.7 % ± 7.4 %).

316 The above validation analyses indicate highly accurate decomposition during the rapid phase of explosive
317 contractions.

318 *Neural Drive and Force*

319 Figures 1B-C and 3 show the discharge timings obtained from the decomposition analysis during the
320 isometric explosive contractions for two representative subjects. The average neural drive across all subjects
321 is reported in Figure 4. The discharge patterns were similar for all the identified motor units (Figs. 1,3). The
322 average recruitment threshold across all subjects was 2.10 (2.46) %MVF. The classic onion-skin scheme
323 (inverse dependency of motor unit recruitment thresholds and firing rate) that is usually observed during
324 controlled isometric force contractions at low forces (De Luca & Erim, 1994) was not observed during the
325 explosive contractions (Fig. 1,2). Indeed, the average speed of recruitment of the identified motor units was
326 extremely high (6.48 (4.74) ms, i.e. on average one motor unit was recruited every 6.48 ms), indicating full
327 recruitment of the identified motor units within 54.3 (30.8) ms. Because of the very fast recruitment, the
328 average discharge rate across the contraction for the first and last recruited motor units did not differ (42.85
329 (10.19) vs. 41.55 (11.58), (pps), Paired T-test P = 0.57). Consequently, the association between motor unit
330 recruitment thresholds and the DR_{MEAN} (either during the neuromechanical delay or averaged along the
331 contraction) was not significant ($R^2 = 0.09$, $P>0.05$).

The maximal motor unit discharge rate (DR_{MAX}), from amongst all the motor units from all the participants, ranged from 8.56 to 227.6 pps. The strength of the neural drive to the muscle decreased over time (Figure 4) and was significantly greater during the initial phase of the contraction when compared to the plateau of the explosive contraction (within the neuromechanical delay, 43.23 (8.69) vs. force plateau 33.40 (7.71), paired T-test, $p<0.001$, Fig. 3).

The maximal instantaneous discharge rate and the strength of the neural drive in the first 35 ms of contraction well explained the ability to generate explosive force. Both the absolute and relative RFD0-X_{MAX} and Impulse were indeed highly correlated with DR_{MAX} during this initial 35-ms interval (average across absolute and normalized RFD values, $R^2 = 0.64$ (0.13) Pearson-$P<0.0001$, Fig. 5). Similarly, DR_{MEAN} during this initial period predicted both the absolute and normalized values of RFD0-X_{MAX} (average across absolute and normalized RFD values $R^2 = 0.62$ (0.09) Pearson-$P<0.001$, Fig. 5). The correlation with the RFD over fixed time periods (60 and 100 ms) was also strongly correlated with the maximal instantaneous discharge rate and the average number of discharges per motor unit per second (average across absolute and normalized RFD0-60/100 ms values, $R^2 = 0.68$ (0.05) $P<0.001$).

Interestingly, none of the neural variables at time intervals following the first 40 ms of motor neuron activity predicted the explosive force estimates (Pearson-$P >0.05$). This indicates that the explosive force was determined exclusively by the initial burst of motor neuron activity, occurring before force generation.

The speed of recruitment of the identified motor units was significantly correlated to the normalized and absolute Impulse and RFD0-X_{MAX} ($R^2 = 0.40$ (0.06), $P<0.05$, Fig 5E). This correlation indicates that subjects with greater explosive force production recruited motor units in shorter time intervals (faster recruitment). Moreover, the speed of recruitment was significantly correlated to DR_{MEAN} and DR_{MAX} ($R^2 = 0.54$ (0.1), Pearson-$P<0.05$, Fig. 5F), indicating that subjects with high discharge rates had also a faster motor unit recruitment. For example, the subject with the highest normalized rate of force development (and discharge rate) had a time span of recruitment as small as ~3 ms that was approximately five times shorter than for the subject with the smallest RFD0-X_{MAX} (~16 ms).

Absolute and normalized EMG amplitude (within the same time intervals used for the neural drive) were uncorrelated to RFD0-X_{MAX} (average $R^2 = 0.38$ (0.32), Pearson-$P>0.05$). Moreover, neither the absolute nor

normalized EMG were significantly correlated with any of the explosive force measurements (R^2 < 0.24, Pearson-P>0.05).

Discussion

We examined the behaviour of a relatively large population of motor neurons during rapid (explosive) contractions. We show for the first time that both the recruitment speed and discharge rate of motor neurons dictate the variability in human rate of force development. Moreover, the presented results suggest that the maximal rate of force development is associated with the cortical drive received by the motor neurons before force and the associated afferent feedback are generated.

Neural drive to muscle and maximal rate of force development

The discharge rate of motor neurons was significantly higher during the first 35 ms of activity than in the subsequent time interval (Figs. 1-3). Because the initial phase of a feedforward task reflects only the efferent drive, the discharge activity of the motor units represents a transformation of the cortical input by the motor neurons. Most motor neurons started discharging before the rise in force (Figures 1 and 2). The activity of the upper motor neurons determines the all-or-none response of the lower motor neurons, thus a faster recruitment of neurons within the cerebral cortex may be the mechanism resulting in a more compressed recruitment of spinal motor neurons for subjects achieving higher rate of force developments.

The underlying determinants for the large range of maximal motor neuron discharge rates across subjects are unknown. Some subjects achieved frequencies in single motor units greater than 160 pps, with one subject reaching frequencies of 200 pps and a force impulse almost two-fold compared to subjects with motor neurons discharging at <100 pps (Fig 4A-B). These differences may be determined by intrinsic characteristics of the motor neuron and/or by corticospinal input strength.

The association between the average discharges per motor unit per second and the recruitment speed of motor neurons reveals the transmission of cortical input by the motor neuron pool. When the central nervous system requires maximal speed, it projects strong synaptic input to the full pool of motor neurons, determining both fast recruitment and high discharge rates. It has been speculated that motor unit recruitment may not be a determinant of maximal feedforward force (Duchateau & Baudry, 2014). However,

386 we observed that a greater number of discharges per motor unit per second is associated with a faster motor
387 unit recruitment and thus to a greater maximal rate of force development. It might be argued that also a more
388 distributed common input to motor neurons could contribute to an increase in motor unit synchronization and
389 rate of force development (Semmler, 2002). However, the association between motor unit synchronization
390 and rate of force development may not be strong (Farina & Negro, 2015).

391 The generated explosive force was determined by a fast increase in synaptic input to motor neurons that
392 determined both a fast recruitment and high discharge rates. The two mechanisms cannot be separated
393 since both depend on the input to the motor neuron pool. This characteristic of motor neurons has been
394 observed also in in-vitro studies when injecting high currents in the motor neuron (Granit *et al.*, 1963). The
395 initial motor neuron discharge rate is associated to the strength of the injected current (Granit *et al.*, 1963).
396 The strength of corticospinal inputs required for explosive force presumably determines the high initial
397 discharge rate of the motor neurons. The non-linear decrease in the discharge rate observed in this study
398 matches well the spike frequency adaptation observed in-vitro in individual motor neurons (Granit *et al.*,
399 1963; Sawczuk *et al.*, 1995), which is associated to the inactivation of Na^+ conductance (Miles *et al.*, 2005).
400 Sawczuk and colleagues showed that the spike frequency adaptation of rat motor neurons follows a rapid
401 decrease in discharge rate, followed by a linear and exponential decline (Sawczuk *et al.*, 1995). Taken
402 together, these results suggest that the corticospinal input strength determines the human variability in
403 explosive force. Moreover, they show a strong correspondence between the in vitro and in vivo findings with
404 the present proposed technique.

405 Recently, motor unit recruitment speed was assessed indirectly via muscle fiber conduction velocity
406 (Andreassen & Arendt-Nielsen, 1987; Del Vecchio *et al.*, 2017) during explosive contractions in a group of
407 controls and chronic strength trained individuals (Del Vecchio *et al.*, 2018*b*). Muscle fiber conduction velocity
408 was associated to maximal rate of force development in both groups but only in the early rise of force (first
409 50 ms). This evidence supports the direct association between motor unit recruitment speed and rate of
410 force development reported in the present study and further highlights the importance of compressing motor
411 unit recruitment range as fast as possible (Del Vecchio *et al.*, 2018*b*).

412 The onion-skin phenomenon that is commonly observed during slowly increasing ramp contractions (De
413 Luca & Erim, 1994), was not observed in the present study, neither during the neuromechanical delay nor,
414 and more interestingly, in the steady phase of the explosive task (Figs. 1-2). This observation is related to

the compressed recruitment of motor neurons and to the high rate of force development. It may thus be argued that the onion skin depends on the slow generation of force. The very short interval of recruitment indicates the possibility that the onion-skin during slow force contractions may be partly determined by the afferent feedback to the motor neurons.

It is interesting to note that the relative and absolute explosive force values were correlated with the neural estimates assessed only during the first 35 ms from the onset of the first detected motor unit action potential. This indicates that it is the initial neural drive sent to the muscles that influences the time course of the explosive contraction. Thus, the neural and contractile factors that have been found to influence explosive force production (Folland *et al.*, 2014) may in fact be intrinsically linked. The relation between absolute explosive force and neural drive may underlie an association between the neural stimulus and adaptation of the muscle fiber contractile properties. It has been commonly observed that the neural activation indeed influences the adaptation of the muscle fibres (Dubowitz, 1967). Although we did not measure fibre contractile properties in this study, the neural determinants of absolute rate of force development may also be associated to corresponding differences in fibre contractility induced by neural activation.

In the present study we revealed the full association between the maximal speed of recruitment and discharge rate of motor neurons and explosive contractions of the human tibialis anterior muscle. Interestingly, the proposed technique showed high validity in identifying the same unit across the different phases of the rise in muscular force. The present result shows for the first time the strategies used by the central nervous system to achieve the maximal rate of force development. The proposed methodological approach of HDsEMG decomposition can be used to test non-invasively the maximal discharge rate of motor neurons, therefore it allows to study the chronic and acute changes of the neural and muscular function. The results from the present study indicate that the cortical inputs received by the motor neurons before force is generated dictate our potential to generate force rapidly.

Additional Information

Competing Interests and funding

The authors declare no conflicts of interests. This work was funded by Proof-of-Concept Project Interspine (737570) and the Slovenian Research Agency (project J2-7357 - Exact quantification of muscle control strategies and co-activation patterns in robot-assisted rehabilitation of hemiparetic patients, and Programme

443 funding P2-0041). F. Negro was funded by the European Union's Horizon 2020 research and innovation
444 programme under the Marie Skłodowska-Curie grant agreement No 702491 (NeuralCon). The authors
445 declare no competing financial interests.

446 *Author contributions*

447 All authors contributed to the conception and design of the work. ADV and AC acquired the data. ADV, FN,
448 AH, and DF analysed the data. ADV drafted the manuscript and plotted the figures. All authors contributed to
449 the interpretation of the results and in the revision of the manuscript. All authors have approved the final
450 version of the submitted manuscript for publication and are accountable for all aspects of the work. All
451 persons designated as authors qualify for authorship, and all those who qualify for authorship are listed.

452

453 **Reference**

454 Aagaard P, Simonsen EB, Andersen JL, Magnusson P & Dyhre-Poulsen P (2002). Increased rate of force
455 development and neural drive of human skeletal muscle following resistance training. *J Appl Physiol*
456 **93,** 1318–1326.

457 Andreassen S & Arendt-Nielsen L (1987). Muscle fibre conduction velocity in motor units of the human
458 anterior tibial muscle: a new size principle parameter. *J Physiol* **391,** 561–571.

459 Büdingen HJ & Freund HJ (1976). The relationship between the rate of rise of isometric tension and motor
460 unit recruitment in a human forearm muscle. *Pflügers Arch Eur J Physiol* **362,** 61–67.

461 Van Cutsem M & Duchateau J (2005). Preceding muscle activity influences motor unit discharge and rate of
462 torque development during ballistic contractions in humans. *J Physiol* **562,** 635–644.

463 Van Cutsem M, Duchateau J & Hainaut K (1998). Changes in single motor unit behaviour contribute to the
464 increase in contraction speed after dynamic training in humans. *J Physiol* **513,** 295–305.

465 Desmedt JE & Godaux E (1977*a*). Fast motor units are not preferentially activated in rapid voluntary
466 contractions in man. *Nature* **267,** 717–719.

467 Desmedt JE & Godaux E (1977*b*). Ballistic contractions in man: characteristic recruitment pattern of single
468 motor units of the tibialis anterior muscle. *J Physiol* **264,** 673–693.

469 Desmedt JE & Godaux E (1978). Ballistic contractions in fast or slow human muscles: discharge patterns of
470 single motor units. *J Physiol* **285,** 185–196.

471 Deutekom M, Beltman JG, de Ruiter CJ, de Koning JJ & de Haan a (2000). No acute effects of short-term
472 creatine supplementation on muscle properties and sprint performance. *Eur J Appl Physiol* **82,** 223–
473 229.

474 Dubowitz V (1967). Cross-innervated mammalian skeletal muscle: histochemical, physiological and
475 biochemical observations. *J Physiol* **193,** 481–496.

476 Duchateau J & Baudry S (2014). Maximal discharge rate of motor units determines the maximal rate of force
477 development during ballistic contractions in human. *Front Hum Neurosci* **8,** 9–11.

478 Enoka RM & Duchateau J (2017). Rate coding and the control of muscle force. *Cold Spring Harb Perspect*
479 *Med*; DOI: 10.1101/cshperspect.a029702.

480 Farina D, Arendt-Nielsen L, Merletti R & Graven-Nielsen T (2002). Assessment of single motor unit
481 conduction velocity during sustained contractions of the tibialis anterior muscle with advanced spike
482 triggered averaging. *J Neurosci Methods* **115,** 1–12.

483 Farina D & Negro F (2015). Common Synaptic Input to Motor Neurons, Motor Unit Synchronization, and
484 Force Control. *Exerc Sport Sci Rev* **43,** 23–33.

485 Folland JP, Buckthorpe MW & Hannah R (2014). Human capacity for explosive force production: Neural and
486 contractile determinants. *Scand J Med Sci Sport* **24,** 894–906.

487 Freund H (1983). Motor unit and muscle activity in voluntary motor control. *Physiol Rev* **63,** 387–436.

488 Fuglevand AJ, Winter DA & Patla AE (1993). Models of recruitment and rate coding organization in motor-
489 unit pools. *J Neurophysiol* **70,** 2470–2488.

490 Granit R, Kernell D & Shortess GK (1963). Quantitative aspects of repetitive firing of mammalian
491 motoneurones, caused by injected currents. *J Physiol* **168,** 911–931.

492 de Haan A (1998). The influence of stimulation frequency on force-velocity characteristics of in situ rat medial
493 gastrocnemius muscle. *Exp Physiol* **83,** 77–84.

494 Harwood B & Rice CL (2012). Changes in motor unit recruitment thresholds of the human anconeus muscle
495 during torque development preceding shortening elbow extensions. *J Neurophysiol* **107,** 2876–2884.

Holobar A, Minetto M a & Farina D (2014). Accurate identification of motor unit discharge patterns from high-density surface EMG and validation with a novel signal-based performance metric. *J Neural Eng* **11,** 016008.

Holobar A & Zazula D (2007). Multichannel blind source separation using convolution Kernel compensation. *IEEE Trans Signal Process* **55,** 4487–4496.

Klass M, Baudry S & Duchateau J (2008). Age-related decline in rate of torque development is accompanied by lower maximal motor unit discharge frequency during fast contractions. *J Appl Physiol* **104,** 739–746.

De Luca CJ & Erim Z (1994). Common drive of motor units in regulation of muscle force. *Trends Neurosci* **17,** 299–305.

Martinez-Valdes E, Farina D, Negro F, Del Vecchio A & Falla D (2018). *Early Motor Unit Conduction Velocity Changes To Hiit Versus Continous Training*. Available at: http://insights.ovid.com/crossref?an=00005768-900000000-96868.

Miles GB, Dai Y & Brownstone RM (2005). Mechanisms underlying the early phase of spike frequency adaptation in mouse spinal motoneurons. *J Physiol* **566,** 519–532.

Negro F, Muceli S, Castronovo AM, Holobar A & Farina D (2016). Multi-channel intramuscular and surface EMG decomposition by convolutive blind source separation. *J Neural Eng* **13,** 026027.

de Ruiter CJ, Vermeulen G, Toussaint HM & de Haan A (2007). Isometric Knee-Extensor Torque Development and Jump Height in Volleyball Players. *Med Sci Sport Exerc*1336–1346.

Sawczuk a, Powers RK & Binder MD (1995). Spike frequency adaptation studied in hypoglossal motoneurons of the rat. *J Neurophysiol* **73,** 1799–1810.

Semmler JG (2002). Motor unit synchronization and neuromuscular performance. *Exerc Sport Sci Rev* **30,** 8–14.

Tanji J & Kato M (1973). Firing rate of individual motor units in voluntary contraction of abductor digiti minimi muscle in man. *Exp Neurol* **40,** 771–783.

Tillin NA, Jimenez-Reyes P, Pain MTG & Folland JP (2010). Neuromuscular performance of explosive power athletes versus untrained individuals. *Med Sci Sports Exerc* **42,** 781–790.

Tillin NA, Pain MTG & Folland JP (2013). Identification of contraction onset during explosive contractions. Response to Thompson et al. “Consistency of rapid muscle force characteristics: Influence of muscle contraction onset detection methodology” [J Electromyogr Kinesiol 2012;22(6):893-900]. *J Electromyogr Kinesiol* **23,** 991–994.

Del Vecchio A, Bazzucchi I & Felici F (2018*a*). Variability of estimates of muscle fiber conduction velocity and surface EMG amplitude across subjects and processing intervals. *J Electromyogr Kinesiol* **40,** 102–109.

Del Vecchio A, Negro F, Falla D, Bazzucchi I, Farina D & Felici F (2018*b*). Higher muscle fiber conduction velocity and early rate of torque development in chronically strength trained individuals. *J Appl Physiol*japplphysiol.00025.2018.

Del Vecchio A, Negro F, Felici F & Farina D (2017). Associations between motor unit action potential parameters and surface EMG features. *J Appl Physiol* **123,** 835–843.

Del Vecchio A, Negro F, Felici F & Farina D (2018*c*). Distribution of muscle fibre conduction velocity for representative samples of motor units in the full recruitment range of the tibialis anterior muscle. *Acta Physiol (Oxf)*; DOI: 10.1111/apha.12930.

Del Vecchio A, Ubeda A, Sartori M, Azorin JM, Felici F & Farina D (2018*d*). Central Nervous System Modulates the Neuromechanical Delay in a Broad Range for the Control of Muscle Force. *J Appl Physiol* **44,** japplphysiol.00135.2018.

Figure Captions

Figure 1. A. Representative example of the motor neuron discharge timings from the spinal cord with the resultant force output. **B.** Twenty-two motor units identified during an explosive contraction normalized to maximal voluntary force (MVF, in grey). **C.** The discharge rate of the motor units shown in A. The orange line corresponds to the average number of discharges per motor unit per second (during a moving 35 ms time interval), which is an estimate of the neural drive to the muscle.

Figure 2. Explosive force estimates. Each colour corresponds to a specific subject. **A-B** The force-time curve in newtons (N) and normalized to maximal voluntary force (%).**C-D** Absolute and normalized values of the force-time integral. **E-F** The maximal rate of force development (RFD0-X_{MAX}) to the highest gradient from onset to each point up the rising curve in absolute and normalized (to MVF) terms. The peak of the maximal

rate of force development was inversely correlated with time. Correlation coefficients (R^2) and P values are given. ** P < 0.001

Figure 3. A-B Three maximal explosive force contractions (grey lines). Each colour represents the same motor unit tracked during these contractions. The motor unit pulse train were identified by blind source separation of the high-density surface electromyogram. **C.** The discharge timings of the motor unit 1 in **A** (corresponding to the red circle with white fill) were used as triggers for the extraction of the motor unit signature shown in C. In this example, the signatures were extracted by spike triggered averaging the first twenty discharges (in green). The action potential waveform was then correlated to the signature extracted from the last fifty discharges (during the plateau, in red) of the explosive contraction. **D.** The signature of motor unit 5 (black circle with white fill) in **A** was correlated across the three contractions. It can be noted the high degree of similarity between the motor unit action potential within and between contractions.

Figure 4. The average number of discharges per motor unit per second, which is an estimate of the neural drive to the muscle (DR_{MEAN}, pps) and the explosive contractions (in percentages of maximal voluntary force) when averaged across subjects. The dotted lines correspond to the mean, and the edges of the shaded plot to the standard deviation. It can be noted the peak of the neural drive corresponding to the initial phase of the explosive force contraction.

Figure 5. Scatter plots showing the associations between explosive force estimates and motor unit activity. **A-B** The normalized and absolute force-time Integral (Impulse, from onset to 250 ms) in relation to the maximal instantaneous discharge rate that was obtained in the first 35 of motor unit activity. Each colour represents one subject. **C-D.** The average number of discharges per motor unit per second during the first 35 ms of motor unit activity (DR_{MEAN}) in relation to the absolute and normalized maximal rate of force development (RFD0-X_{MAX}). The RFD0-X_{MAX} represents the peak of the force derivative. **E-F** The maximal discharge rate of the motor neurons in relation to the rate of force development from onset to 100 ms (RFD0-100). **G.** The time force integral (Impulse, N*s) when plotted as a function of the motor unit recruitment speed (Motor units/s). **H**. Association between the maximal discharge rate of motor neurons (DR_{MAX}) and motor unit recruitment speed (Motor units/s). The motor unit recruitment speed corresponds to the average number of identified motor units per second. R^2 values for each relationship are shown and *** indicates P < 0.0001.

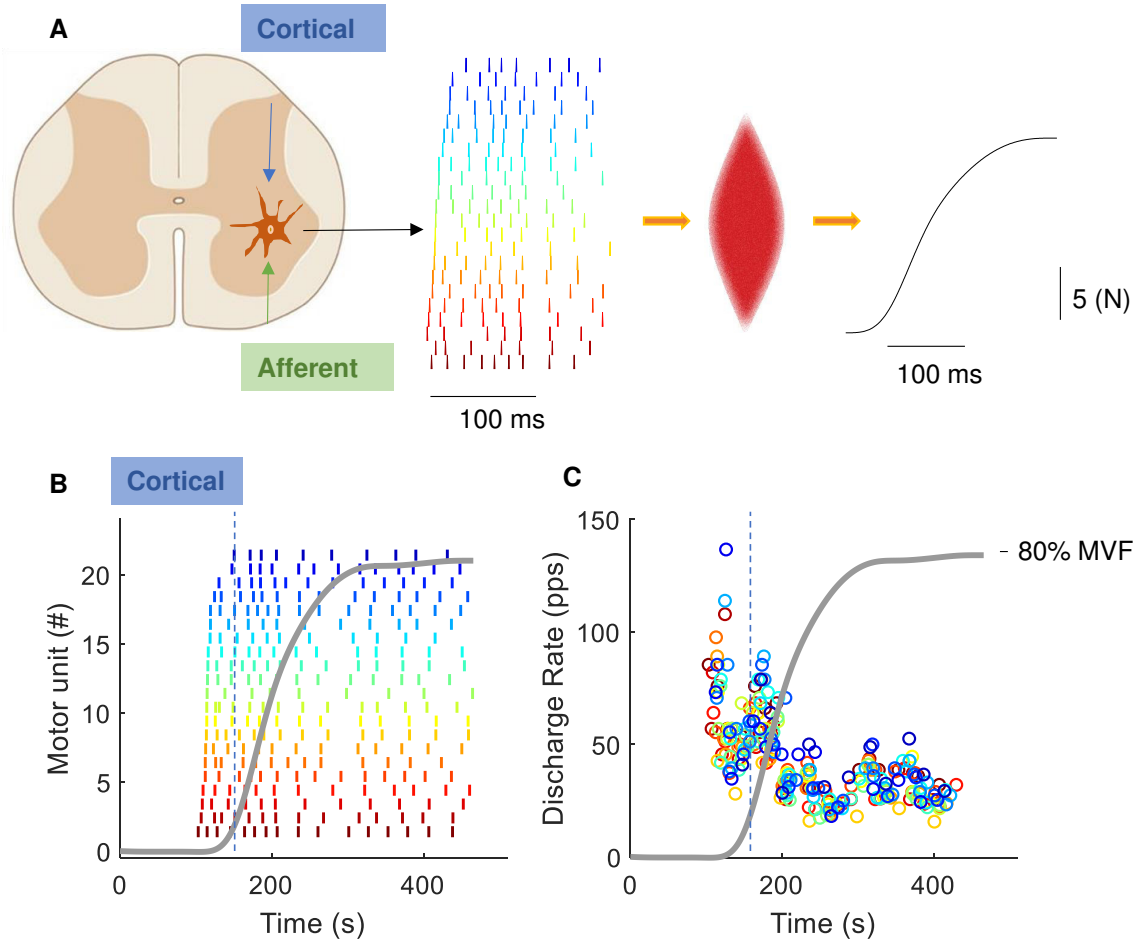
A
Cortical
Afferent
100 ms
5 (N)
100 ms
B
Cortical
Motor unit (#)
Time (s)
C
Discharge Rate (pps)
80% MVF
Time (s)

Figure 1

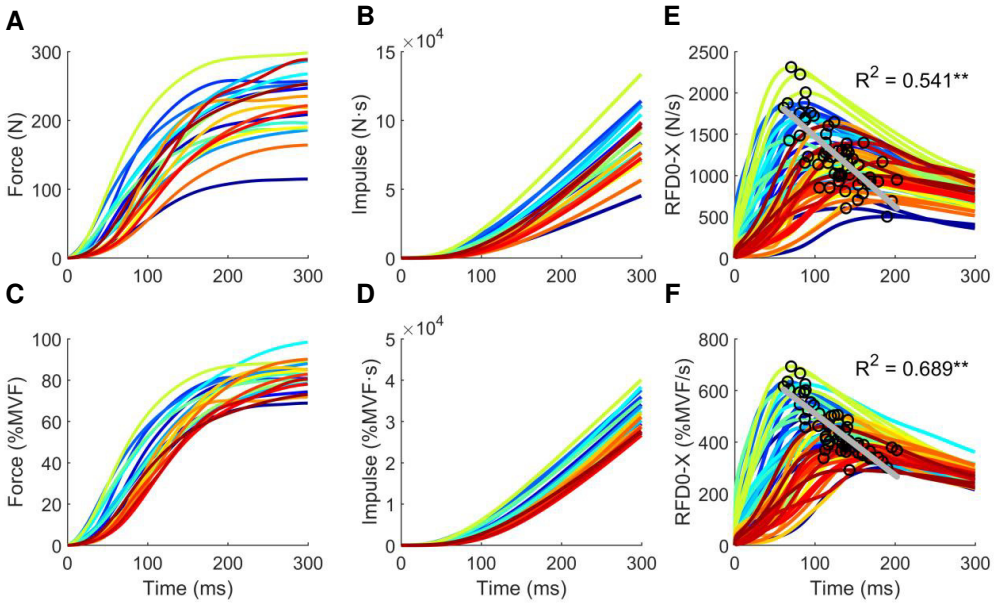
A
B
E
C
D
F
Force (N)
Impulse (N·s)
RFD0-X (N/s)
Force (%MVF)
Impulse (%MVF·s)
RFD0-X (%MVF/s)
Time (ms)
Time (ms)
Time (ms)
×10^4
×10^4
R^2 = 0.541**
R^2 = 0.689**

Figure 2

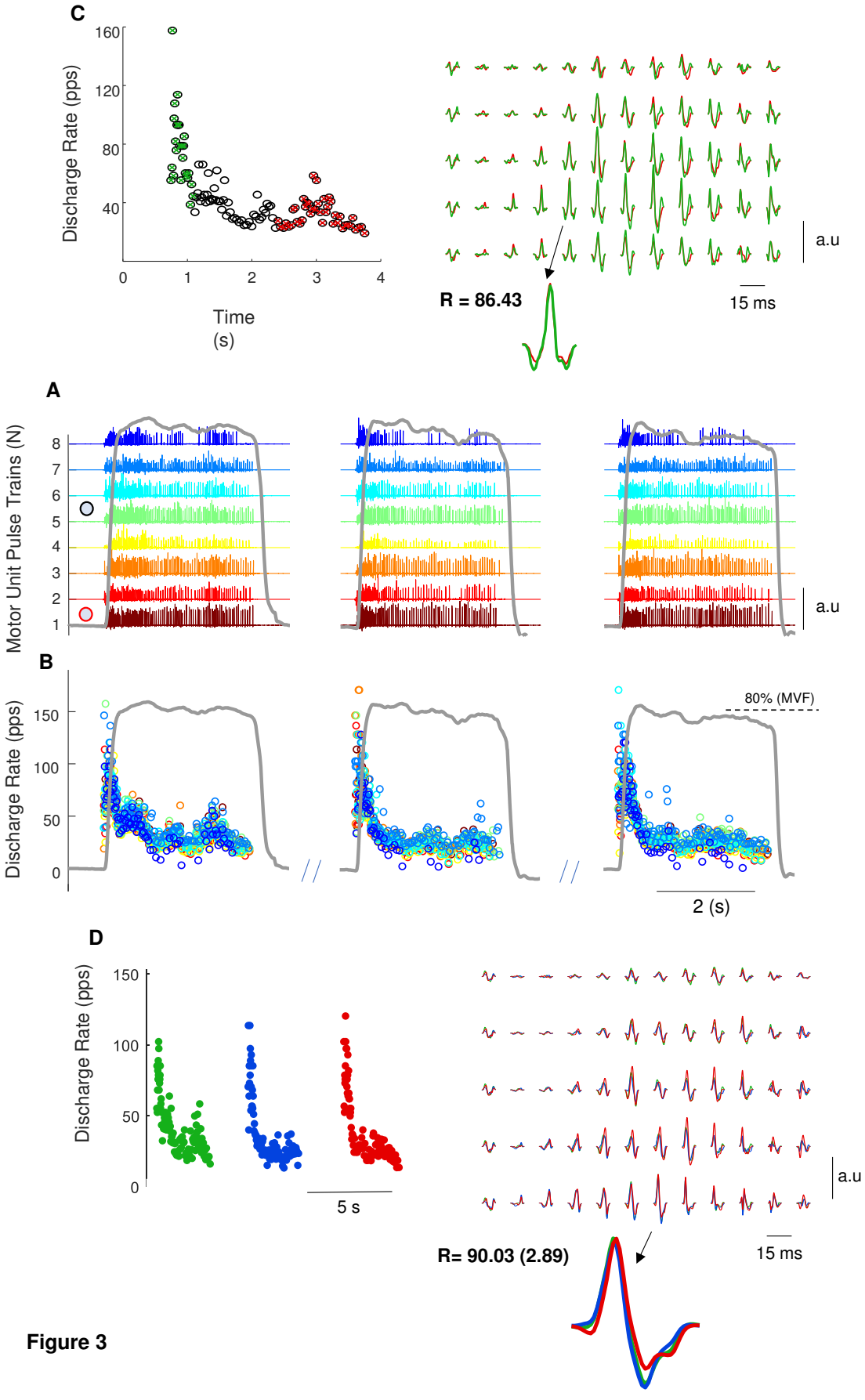
C
Discharge Rate (pps)
160
120
80
40
0
1
2
3
4
Time
(s)
a.u
R = 86.43
15 ms
A
Motor Unit Pulse Trains (N)
8
7
6
5
4
3
2
1
a.u
B
Discharge Rate (pps)
150
100
50
0
80% (MVF)
2 (s)
D
Discharge Rate (pps)
150
100
50
0
5 s
a.u
R= 90.03 (2.89)
15 ms

Figure 3

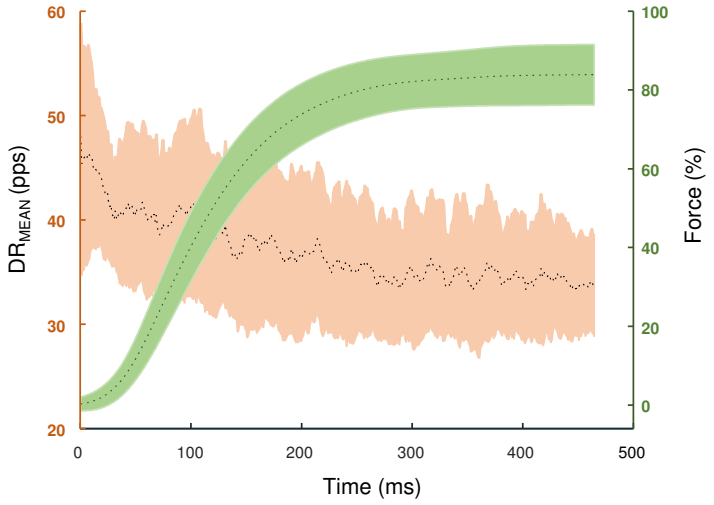
60
50
40
30
20
DR_MEAN (pps)
100
80
60
40
20
0
Force (%)
0
100
200
300
400
500
Time (ms)

Figure 4

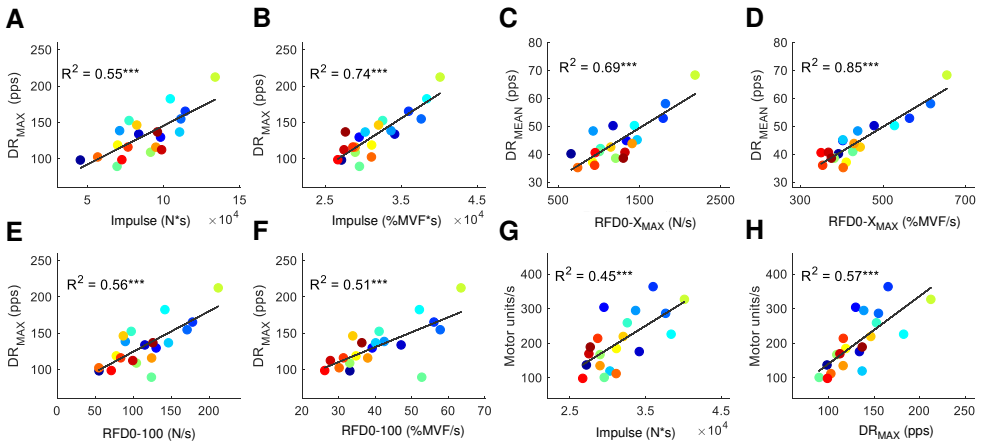
A
B
C
D
E
F
G
H
R2 = 0.55***
R2 = 0.74***
R2 = 0.69***
R2 = 0.85***
R2 = 0.56***
R2 = 0.51***
R2 = 0.45***
R2 = 0.57***
DRMAX (pps)
DRMEAN (pps)
Motor units/s
Impulse (N*s) ×10^4
Impulse (%MVF*s) ×10^4
RFD0-XMAX (N/s)
RFD0-XMAX (%MVF/s)
RFD0-100 (N/s)
RFD0-100 (%MVF/s)
Impulse (N*s) ×10^4
DRMAX (pps)

Figure 5